nature climate change

LETTERS

PUBLISHED ONLINE: 10 MARCH 2013 | DOI: 10.1038/NCLIMATE1840

Recent multidecadal strengthening of the Walker circulation across the tropical Pacific

Michelle L. L'Heureux[1]*, Sukyoung Lee[2] and Bradfield Lyon[3]

The Pacific Walker circulation is a large overturning cell that spans the tropical Pacific Ocean, characterized by rising motion (lower sea-level pressure) over Indonesia and sinking motion (higher sea level-pressure) over the eastern Pacific[1,2]. Fluctuations in the Walker circulation reflect changes in the location and strength of tropical heating, so related circulation anomalies have global impacts[3,4]. On interannual timescales, the El Niño/Southern Oscillation accounts for much of the variability in the Walker circulation, but there is considerable interest in longer-term trends and their drivers, including anthropogenic climate change[5–12]. Here, we examine sea-level pressure trends in ten different data sets drawn from reanalysis, reconstructions and *in situ* measurements for 1900–2011. We show that periods with fewer *in situ* measurements result in lower signal-to-noise ratios, making assessments of sea-level pressure trends largely unsuitable before about the 1950s. Multidecadal trends evaluated since 1950 reveal statistically significant, negative values over the Indonesian region, with weaker, positive trends over the eastern Pacific. The overall trend towards a stronger, La Niña-like Walker circulation is nearly concurrent with the observed increase in global average temperatures, thereby justifying closer scrutiny of how the Pacific climate system has changed in the historical record.

The Pacific Walker circulation is a key component of the global atmospheric circulation and its variability is associated with precipitation and temperature variations over disperse regions of the planet[3,4,13]. Its signature east–west sea-level pressure (SLP) differences across the tropical Pacific are linked with ascending motion and deep convection over the warm water surrounding Indonesia, contrasting with subsidence and net radiative cooling over the cooler water of the eastern Pacific Ocean[1,2]. Owing to the interrelationships between SLP, tropical rainfall[14], winds[15] and sea surface height[16], studies assessing variability and trends in the Walker circulation extend beyond evaluations of SLP alone. Yet the surface expression of pressure is a fundamental aspect of the Walker circulation, with SLP records central to the studies by its namesake, Sir Gilbert Walker, when exploring the linkages between the South Asian monsoon and the tropical Pacific circulation back in the early twentieth century[17].

Most coupled model simulations reveal SLP trends indicative of a weakened Walker circulation over the twentieth century[5,8,11]. This weakening has been attributed to warming by anthropogenic greenhouse gases, which increases water vapour by roughly 7% $°C^{-1}$, in agreement with the Clausius–Clapeyron relationship. These models also show precipitation increases at a slower rate of ~2–3% $°C^{-1}$ (refs 8,9). As latent heat associated with precipitation must balance radiative cooling in the global tropics, the Walker circulation in the models must slow down to compensate for the differential rates between water vapour and precipitation[18]. In contrast, some studies suggest the observed rate of change of precipitation and evaporation is larger, on par with the increase in water vapour[10,19], and thus not necessitating a compensating decrease in the overturning circulation. Although precipitation trends, particularly over ocean areas, are hampered by relatively short observational records that disagree[20–23], longer proxy records, such as ocean salinity, indicate a strong freshening of water over the western Pacific warm pool during 1950–2000, suggesting a stronger hydrological response (~8% $°C^{-1}$; ref. 24).

Although model simulations of a weakened Walker circulation have been corroborated in a few observational SLP data sets[5,11,12], a more expansive comparative analysis of the data, and *in situ* data coverage, has not been undertaken so far. *In situ* SLP observations over the tropical Pacific vary greatly in space and time, posing challenges to both the robust evaluation of associated trends and validation of climate model simulations[25]. Some recent papers examined a single, least-squares linear trend over the full SLP record[11,12,26], or used model simulations forced by observed sea surface temperatures (SSTs) to determine the resulting SLP trends[6,12]. Here, we examine ten different, observation-based SLP data sets drawn from various reconstructions, reanalysis and *in situ* records to evaluate their quality over the Indo-Pacific region (see Supplementary Methods for the data sets used). To minimize the influence of end points, temporal trends are computed every six months over moving 10-, 20-, 30- and 40-year temporal windows in each data set starting in January 1900 to December 2011. Figure 1 shows the running linear trends of SLP over the Indonesia–Pacific warm pool region (110°–160° E, 10° S–10° N) and the eastern Pacific Ocean (130°–80° W, 10° S–10° N) for each data set (black line depicts the average of all data sets). Supplementary Fig. S1 shows the same data as in Fig. 1, but provides a close-up for the satellite-era record (1979–2011). Trends based on the single *in situ*-alone data set, the International Comprehensive Ocean–Atmosphere Data Set (ICOADS), are shown but excluded from the data set average because of the lack of quality control and amount of missing data. Also, only well-sampled grid boxes in ICOADS are used to form regional SLP trends (see Methods), whereas others have used linear interpolation to infill missing data[12]. However, particularly during the recent record, our trend estimate from ICOADS compares relatively well to the other data sets, which lends support to the primary results.

From Fig. 1, we see that linear SLP trends based on the 10-year window exhibit no consistent tendency over Indonesia and

[1]NOAA Climate Prediction Center, 5830 University Research Court, Room 3115, College Park, Maryland 20740, USA, [2]Meteorology and Atmospheric Science, Pennsylvania State University, 524 Walker Building, University Park, Pennsylvania 16802, USA, [3]International Research Institute for Climate and Society, PO Box 1000, 110 Monell Building, Palisades, New York 10964, USA. *e-mail: michelle.lheureux@noaa.gov.

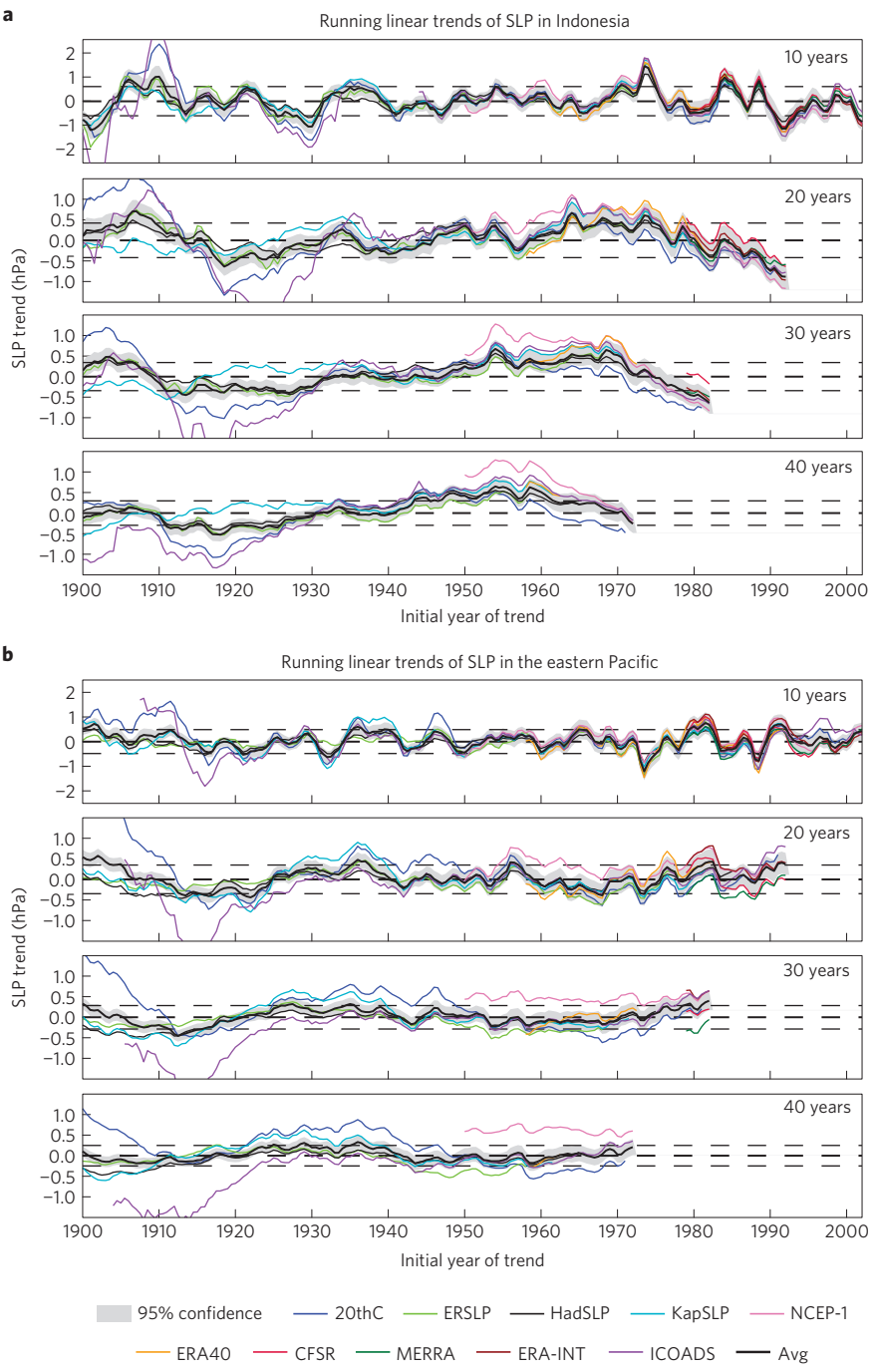

Figure 1 | SLP linear trends for 10-, 20-, 30-, 40-year moving windows from January 1900 to December 2011. a,**b**, Trends for the region over Indonesia (110°–160° E, 10° S–10° N; **a**) and for the region over the eastern Pacific Ocean (130°–80° W, 10° S–10° N; **b**) . SLP is expressed as the change (hPa) over the window length. Grey shading represents the 95% confidence level based on a two-tailed Student's *t*-test. The dashed, horizontal lines represent the 95% range of trends based on 1,000 synthetic AR(1) time series. The *x* axis shows the initial year of the trend (for 10-year windows, 1950 denotes the 1950–1959 trend).

the eastern Pacific. However, over Indonesia, longer timescale trends become more apparent in the 20–40-year windows. Starting in 1910–1920, a gradual increase from negative to positive trends is discernible there. Then beginning in 1955–1965, the increasing positive trends stall and subsequently the slope becomes strongly negative with a ~1–1.5 hPa decrease occurring in recent decades. Thus, although the trend over Indonesia is negative after 1970–1980, depending on the window length, the earlier positive trends begin to weaken a decade or so before then. Over the eastern Pacific, SLP multidecadal trends are not as unequivocal or significant, but there are hints of an increasing tendency towards more positive trends starting in the late 1950s or 1960s. This positive tendency becomes clearer after the SLP relationship with the El Niño/Southern Oscillation (ENSO) is linearly removed (discussed later in the text). Overall, the multidecadal tendency towards lower SLP over Indonesia and higher SLP over the eastern Pacific suggests a strengthening Walker circulation during the last half of the twentieth century.

Despite the century-length record, the data before the ~1950s are fraught with issues and are very likely unreliable for trend

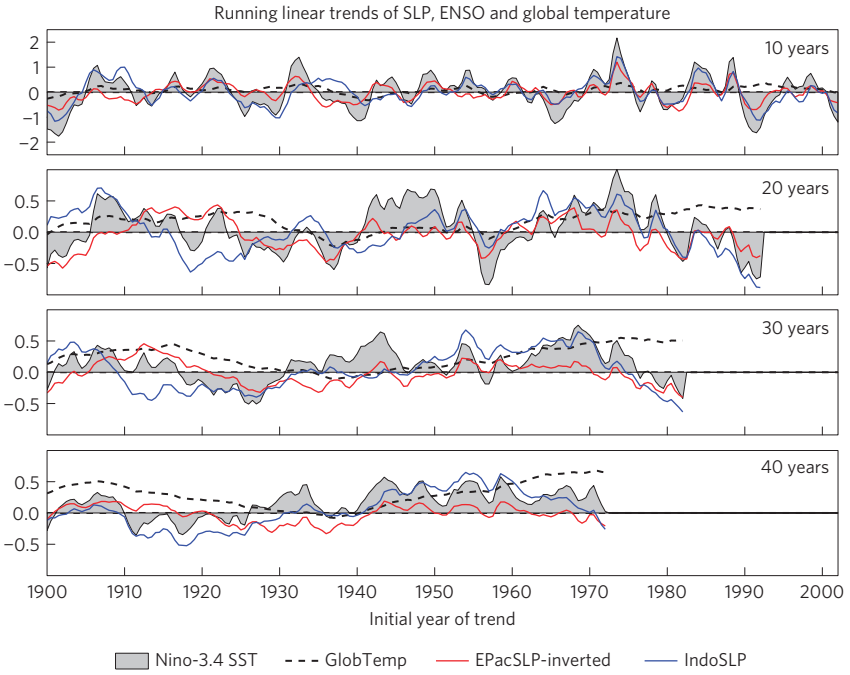

Figure 2 | SLP linear trends over the eastern Pacific Ocean and over Indonesia for 10-, 20-, 30- and 40-year moving windows for January 1900–December 2011. Trends are shown for Niño-3.4 SST (grey shading) and global temperature (black dashed). SLP trends are based on the average of all available data sets (excluding ICOADS) and expressed as the change (hPa) over the window length. Niño-3.4 SST and global average temperature are the change (°C) over the window length.

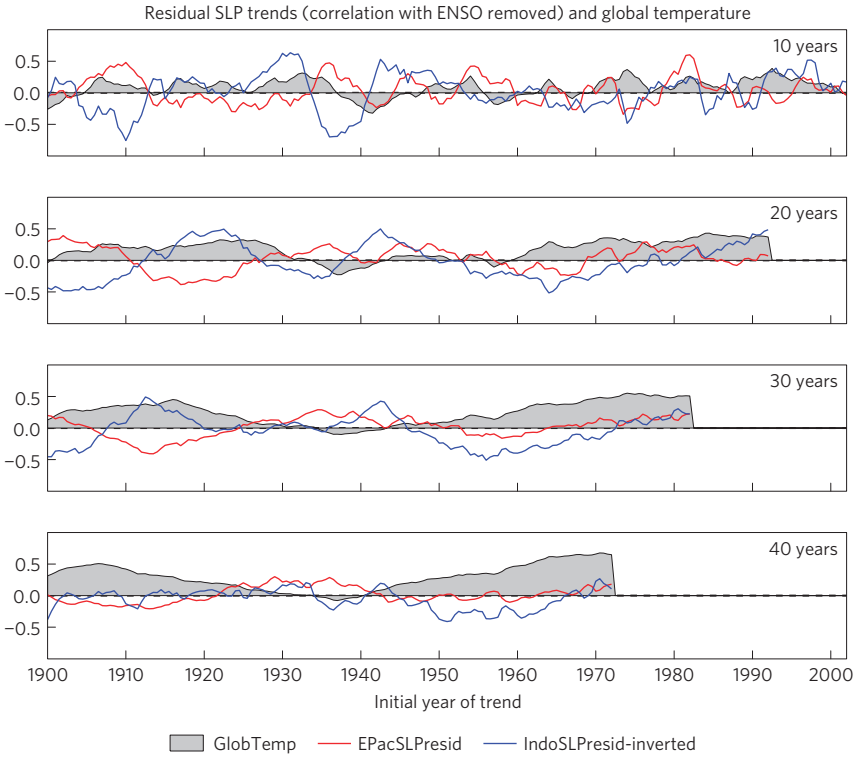

Figure 3 | Residual SLP trends, with Niño-3.4 SST linearly removed, over the eastern Pacific Ocean and over Indonesia for 10-, 20-, 30- and 40-year moving windows for January 1900–December 2011. Grey shading indicates trends for global temperature. SLP trends are based on the average of all available data sets (excluding ICOADS) and expressed as the change (hPa) over the window length. Niño-3.4 SST and global average temperature are the change (°C) over the window length.

analysis. In particular, the ICOADS *in situ* data set, which is a key component of the other reconstructions and reanalysis, has a pronounced lack of data in the two regions during the first half of the twentieth century (Supplementary Fig. S2). In that period the spatial coverage of gridded *in situ* observations in each region is less than 50% and, for some periods, is closer to the 0–25% range

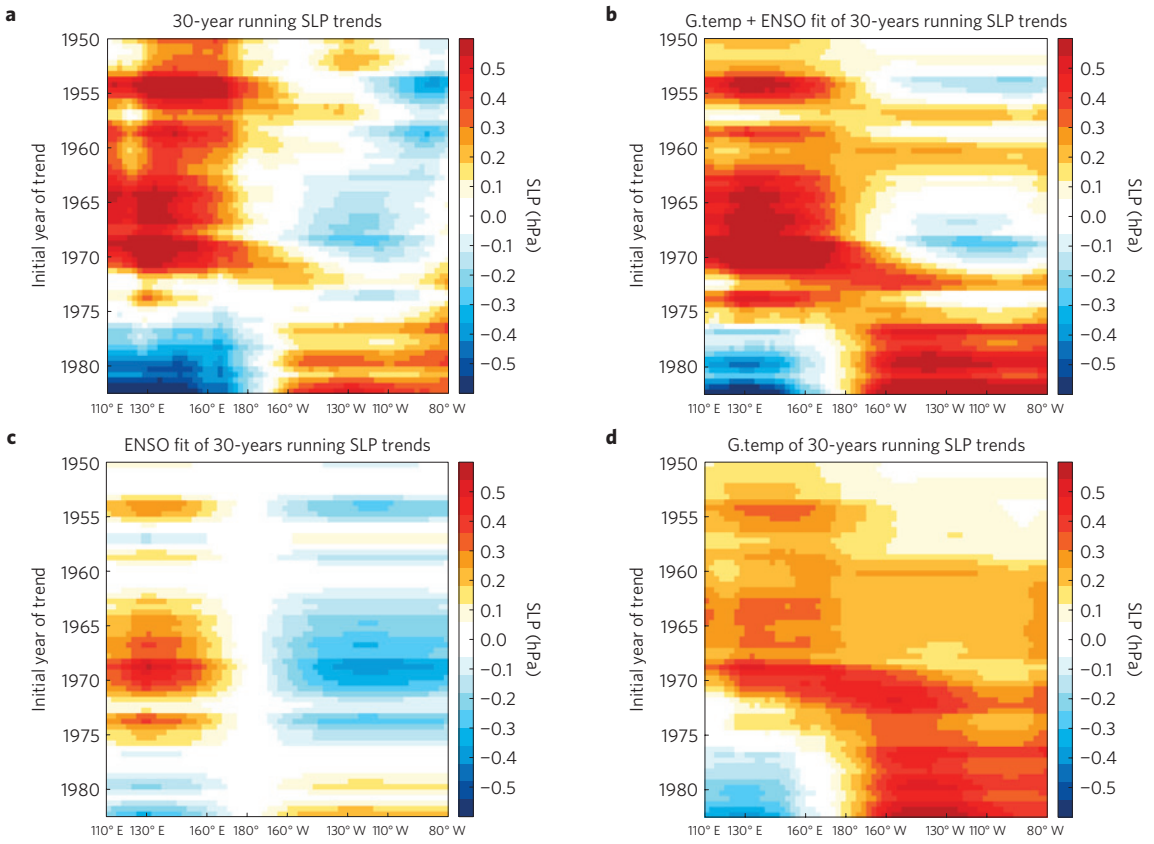

Figure 4 | Hovmoller diagrams of 30-year moving SLP linear trends, averaged between 10° S and 10° N, across the tropical Indo-Pacific Ocean. **a**, Observed moving SLP trends based on the average of all available data sets (excluding ICOADS). **b**, Sum of the SLP trends based on the fits shown in **c**,**d**. **c**, SLP trends fitted to the Niño-3.4 SST index. **d**, SLP trends fitted to the global average temperature index (which has the Niño-3.4 SST index linearly removed). SLP is expressed as the change (hPa) over the 30-year window.

(Supplementary Fig. S3). The consequences of the deficiency of *in situ* data become clearer when the *in situ* coverage of ICOADS is compared with the signal-to-noise (S/N) ratio of the remaining data sets (Supplementary Fig. S4; see Methods for calculation). In general, the reliability of the data set average (black line in Fig. 1) improves when the S/N is greater than one. Before 1960, the S/N ratio for large portions of the Pacific is less than one, reflecting the disagreement among data sets. This low ratio corresponds closely to the dearth of ICOADS coverage at each longitude (for 10° S–10° N). After 1960, both the coverage and the S/N ratios markedly improve, although they are still relatively low over the central Pacific (160° E–120° W).

As mentioned, variability in the Walker circulation is closely tied to ENSO (refs 1,3,4), although it is suggested that longer-term trends are linked to the increase in global mean temperatures[5,7–9]. To visualize how these two factors contribute to the SLP trends, the data set average SLP trends are superimposed against trends in the Niño-3.4 (ref. 26) SST index, representing the ENSO, and the global average temperature (Fig. 2). For the 10-year moving trends, it is clear that SLP trends in the eastern Pacific (inverted in the figure) and Indonesian region are nearly synchronous with decadal variability in ENSO. Disagreement between ENSO and the regional SLP trends increases slightly for the 20–40-year trends, and is particularly visible in the pre-1950 record manifest by larger excursions of the SLP trends outside the shaded region representing ENSO. After 1950, the tendency in multidecadal Niño-3.4 trends is largely positive and then becomes negative starting in the early 1970s, which is generally mirrored by the SLP trends.

To further elucidate the linkage of global mean temperature to SLP trends, ENSO is linearly removed from the regional SLP trends (using the Niño-3.4 index[26]). Previous studies have used other techniques to extract the influence of ENSO (refs 27,28). The results (Fig. 3) show, for the 20–40-year windows, increasing SLP trends over Indonesia (now inverted) and the eastern Pacific, as the positive global mean temperature trend emerges after mid-century. Although the SLP trends do not identically share the same sign as the temperature trends, the implied strengthening of the Walker circulation seems to be consistent with the increasing, positive trend in global mean temperatures. Also revealing is the conspicuous shift in the behaviour of the regional SLP trends in the various data sets after the ~1950s when they come into greater agreement. Earlier, the SLP trends are clearly not in sync, and given the known scarcity of data during this period, this result also calls into question the reliability of trends that include the earlier historical record, as in previous studies.

The contribution of ENSO and the global mean temperature to the average SLP trend across data sets is further broken down in the 30-year moving SLP trends across the tropical Indo-Pacific basin (averaged between 10° S and 10° N) starting in 1950 (Fig. 4). The SLP trends associated with ENSO and the global average temperature are found by calculating trends on linearly fitted SLP anomalies (see Methods). We find that the observed SLP pattern is broadly consistent with both ENSO and global mean temperatures up until the early 1970s. We also find the fitted global temperature SLP trend pattern bears strong similarity to the observed trend pattern after ENSO has been linearly removed (Supplementary Fig. S5). After the early 1970s, the global mean temperature fit begins to clearly dominate the observed pattern of SLP, with negative trends in the western Pacific and positive trends east of the International Date Line. The trends in ENSO are also consistent with the stronger

Walker circulation, but are much weaker and less persistent. Even though ENSO is linearly removed from the global temperature index, the sum of the two fitted trends is slightly larger than for the full observations. It is likely that the summation results in slight double counting due to nonlinear relationships between ENSO and global temperature. However, the spatial similarity between the summed, fitted patterns and observations is remarkable and demonstrates that SLP trends since the ~1950s are nearly entirely driven by the linear combination of global temperatures and ENSO.

These results demonstrate that the observed Indo-Pacific basin SLP trends are increasingly related to the global mean temperature with time, and that this multidecadal signal is opposite to the model-simulated weakening of the Walker circulation[5,7–9,11,12]. This strengthening may reflect the dominance of internal multidecadal variability over the externally forced anthropogenic signal. However, given its relationship with the trend in global temperature, which presumably is related to the emerging anthropogenic signal, it is also likely that aspects of the model simulations may not be realistic. As implied by some observational studies, it is possible that tropical precipitation trends are underestimated in climate models in response to anthropogenic forcing. Furthermore, recent research suggests that the atmospheric static stability in the coupled climate models is too high[29]. If the relative rate of increase in static stability is less than that in precipitation, the Walker circulation can strengthen. In addition, the ocean dynamical thermostat hypothesis[30] could become a factor if the eastern Pacific upwelling region warms more slowly than the rest of the basin; the enhanced SST gradients could result in a strengthening of the Walker circulation.

Will the strengthening trend in the Walker circulation continue as the climate warms further? To answer this question, it is essential to understand the root cause of the long-term SLP trends. However, regardless of the underlying cause the implications of a strengthening Walker circulation may have long-term consequences for the tropical Pacific (for example, continuation of the observed increase in sea level over the western tropical Pacific and decrease over the eastern Pacific[16]), while also extending far beyond the Pacific. An ongoing strengthening of the Walker circulation may portend multidecadal impacts that resemble La Niña, such as increased rainfall over Indonesia, Central America and northern South America, along with drier conditions over the Horn of Africa and the southern tier of the United States.

Methods

Data sets. Trend analysis was performed on ten SLP data sets. The reanalysis data sets, which assimilate observations with a climate model, include the National Centers for Environmental Prediction's (NCEP) Climate Forecast System Reanalysis (CFSR), NCEP/National Center for Atmospheric Research Reanalysis (NCEP-1), National Aeronautics and Space Administration's Modern Era Retrospective Analysis (MERRA), the European Centre for Medium-Range Weather Forecasts (ECMWF) 40 Year Reanalysis (ERA40), the ECMWF Interim Reanalysis (ERA-INT) and the 20th Century Reanalysis (20thC). The reconstruction data sets, which use statistical methods to combine data, are the Met Office Hadley Centre's SLP version 2 data set (HadSLP), Kaplan's SLP data set (KapSLP) and the National Oceanic and Atmospheric Administration's Extended Reconstructed SLP (ERSLP). The only *in situ* data set is the ICOADS release 2.5 based on enhanced statistics and, starting in 2008, is updated with preliminary data in near real-time by the Earth System Research Laboratory (ESRL). On the basis of data set availability, CFSR, MERRA and ERA-INT trends were computed for 1979–2011. Trend calculations are based on 1958–2002 for ERA40, 1950–2011 for NCEP-1, 1900–2004 for HadSLP, 1900–1992 for KapSLP and 1900–1997 for ERSLP. ICOADS and 20thC trends were computed for 1900–2011.

Trend analysis was also performed on the average of two SST data sets and the average of two global average temperature data sets. The SST data sets are the Extended Reconstructed Sea Surface Temperature (ERSST) version 3b and the Hadley Centre Sea Ice and SST (HadISST). The global average temperature (land + ocean) data sets used are the Goddard Institute for Space Studies (GISS) surface temperature analysis (GISTEMP; based on GHCN version 3 and HadISST) and the National Climatic Data Center Historical Merged Land–Ocean surface temperature analysis (based on GHCN-M version 3.1.0 and ERSST version 3b).

All data sets were either originally provided on a 2.5° × 2.5° grid or were interpolated to this grid resolution by using either box averaging (for a less coarse data set as in ERSLP and 20thC) or bilinear interpolation (for a more coarse data set as in KapSLP and HadSLP).

Linear trends. Anomalies are computed as departures from seasonally varying, monthly averages over the entire period the data sets are available, and a least-squares fit is used to calculate the trend. We have provided two significance tests in Fig. 1: a two-tailed Student's t-test (null hypothesis of zero linear trend) with an effective degrees of freedom[31]; the 95% range of trends from 1,000 synthetic AR(1) time series with the same variance and autocorrelations as the original data.

ICOADS trend estimate. ICOADS is *in situ* alone (based on surface marine data) with no spatial interpolation, thus having many missing data points and very minimal quality control. Here, linear trends were calculated by averaging together four different sub-estimates based on monthly data from January 1900 to December 2011: 4 mth yr^{-1}, trend estimates in a grid box are required to have at least 4 months of data within each and every year for the entire record; 6 mth yr^{-1}, similar to 4 mth yr^{-1} except 6 months of data is required; 50%25%, trend estimates in a grid box must have at least 50% of monthly data for the entire record and 25% of monthly data in all of four evenly divided segments of the record; 75%50%, similar to 50%25% except for 75% of data (entire record) and 50% (each segment).

Signal-to-noise ratio. The signal (S) is calculated as the standard deviation of the data set average. The noise (N) is based on the average standard deviation of each individual data set from the data set average. In this instance, S/N ratios are calculated on the SLP anomalies, but S/N could also be calculated on the SLP trends, which can help evaluate whether the trends are significant beyond natural variability. This is practical in a 20thC-type data set with many estimates (56 members; see Supplementary Fig. S6), but not done here because of the lack of ensembles provided with the other observation-based data sets. The use of many independently constructed, ensemble-based data sets could provide assurance that the spread is not model or boundary condition dependent.

Fitted and residual variables. We calculate a fitted variable, $F(t)$, by:

$$F(t) = b \cdot x(t)$$

where b is the regression coefficient or $b = \overline{x'(t)y'(t)}/\overline{x'^2(t)}$. In this paper, $y(t)$ is SLP for a region or at a grid point, and $x(t)$ is the Niño-3.4 or global mean temperature index. A residual time series, which is uncorrelated to $F(t)$ and $x(t)$, is computed by subtracting $F(t)$ from $y(t)$.

In Fig. 4 alone, the global temperature index is first modified by linearly removing the Niño-3.4 index. This removal occurs because global temperatures are correlated with ENSO and we desire to show the fitted SLP trends for ENSO and global temperature separately. However, we note that the residual time series is based on linear, contemporaneous relationships, and therefore does not have lagged or nonlinear relationships removed.

Received 19 September 2012; accepted 30 January 2013; published online 10 March 2013

References

1. Bjerknes, J. Atmospheric teleconnections from the equatorial Pacific. *Mon. Weath. Rev.* **97,** 163–172 (1969).
2. Gill, A. E. Some simple solutions for heat-induced tropical circulation. *Q. J. R. Meteorol. Soc.* **106,** 447–462 (1980).
3. Horel, J. D. & Wallace, J. M. Planetary-scale atmospheric phenomena associated with the Southern Oscillation. *Mon. Weath. Rev.* **109,** 813–829 (1981).
4. Kousky, V. E., Kagano, M. T. & Cavalcanti, I. F. A review of the Southern Oscillation: Oceanic–atmospheric circulation changes and related rainfall anomalies. *Tellus A* **36,** 490–504 (1984).
5. Vecchi, G. A. *et al.* Weakening of tropical Pacific atmospheric circulation due to anthropogenic forcing. *Nature* **441,** 73–76 (2006).
6. Meng, Q. *et al.* Twentieth century walker circulation change: Data analysis and model experiments. *Clim. Dynam.* **38,** 1757–1773 (2012).
7. Knutson, T. R. & Manabe, S. Time-mean response over the tropical Pacific to increased CO_2 in a coupled ocean–atmosphere model. *J. Clim.* **8,** 2181–2199 (1995).
8. Vecchi, G. A. & Soden, B. J. Global warming and the weakening of the tropical circulation. *J. Clim.* **20,** 4316–4340 (2007).
9. Held, I. M. & Soden, B. J. Robust responses of the hydrological cycle to global warming. *J. Clim.* **19,** 5686–5699 (2006).
10. Sohn, B. J. & Park, S-C. Strengthened tropical circulations in past three decades inferred from water vapor transport. *J. Geophys. Res.* **115,** D15112 (2010).
11. DiNezio, P. N., Vecchi, G. A. & Clement, A. C. Detectability of changes in the walker circulation in response to global warming. *J. Clim.* http://dx.doi.org/10.1175/JCLI-D-12-00531.1 (2013).

12. Tokinaga, H., Xie, S-P., Deser, C., Kosaka, Y. & Okumura, Y. Slowdown of the Walker circulation by tropical Indo–Pacific warming. *Nature* **491,** 439–443 (2012).
13. Ropelewiski, C. F. & Halpert, M. S. Precipitation patterns associated with the high index phase of the Southern Oscillation. *J. Clim.* **2,** 268–284 (1989).
14. Lyon, B. & DeWitt, D. G. A recent and abrupt decline in the East African long rains. *Geophys. Res. Lett.* **39,** L02702 (2012).
15. Gastineau, G. & Soden, B. J. Evidence for a weakening of tropical surface wind extremes in response to atmospheric warming. *Geophys. Res. Lett.* **38,** L09706 (2011).
16. Merrifield, M. A. & Maltrud, M. E. Regional sea level trends due to Pacific trade wind intensification. *Geophys. Res. Lett.* **38,** L21605 (2011).
17. Walker, G. T. Correlation in seasonal variations of weather, IX. A further study of world weather. *Mem. India Meteor. Dept.* **24,** 275–333 (1924).
18. Betts, A. K. & Ridgway, W. L. Climatic equilibrium of the atmospheric convective boundary layer over a tropical ocean. *J. Atmos. Sci.* **45,** 2621–2641 (1989).
19. Wentz, F. J., Ricciardulli, L., Hilburn, K. A. & Mears, C. A. How much more rain will global warming bring? *Science* **317,** 233–235 (2007).
20. Allen, M. R. & Ingram, W. J. Constraints on future changes in the hydrological cycle. *Nature* **419,** 224–228 (2002).
21. Allan, R. P. & Soden, B. J. Atmospheric warming and the amplification of precipitation extremes. *Science* **321,** 1481–1484 (2008).
22. John, V. O., Allan, R. P. & Soden, B. J. How robust are observed and simulated precipitation responses to tropical ocean warming? *Geophys. Res. Lett.* **36,** L14702 (2009).
23. Liepert, B. G. & Previdi, M. Do models and observations disagree on the rainfall response to global warming? *J. Clim.* **22,** 3156–3166 (2009).
24. Durack, P. J., Wijffels, S. E. & Matear, R. J. Ocean salinities reveal strong global water cycle intensification during 1950 to 2000. *Science* **336,** 455–458 (2012).
25. Santer, B. D. *et al.* Separating signal and noise in atmospheric temperature changes: The importance of timescale. *J. Geophys. Res.* **116,** D22105 (2011).
26. Barnston, A. G., Chelliah, M. & Goldenberg, S. B. Documentation of a highly ENSO-related SST region in the equatorial Pacific. *Atmos.-Ocean.* **35,** 367–383 (1997).
27. Solomon, A. & Newman, M. Reconciling disparate 20th century Indo–Pacific ocean temperature trends in the instrumental record. *Nature Clim. Change* **2,** 691–699 (2012).
28. Cane, M. A. *et al.* Twentieth century sea surface temperature trends. *Science* **275,** 957–960 (1997).
29. Fu, Q., Manabe, S. & Johanson, C. M. On the warming in the tropical upper troposphere: Models versus observations. *Geophys. Res. Lett.* **38,** L15704 (2011).
30. Clement, A. C., Seager, R., Cane, M. A. & Zebiak, S. E. An ocean dynamical thermostat. *J. Clim.* **9,** 2190–2196 (1996).
31. Bretherton, C. S., Widmann, M., Dymnikov, V. P., Wallace, J. M. & Bladé, I. The effective number of spatial degrees of freedom of a time-varying field. *J. Clim.* **12,** 1990–2009 (1999).

Acknowledgements

We thank Z-Z. Hu and W. Ebisuzaki for their comments and suggestions, and L. Zhang for directing us to some of the data. We also thank NOAA ESRL/PSD and the National Energy Research Scientific Computing Center for providing several data sets on their websites.

Author contributions

All authors contributed to the ideas in this paper. M.L.L. carried out the analysis and wrote the paper. S.L. and B.L. offered their help with interpreting the analysis and also edited the paper.

Additional information

Supplementary information is available in the online version of the paper. Reprints and permissions information is available online at www.nature.com/reprints. Correspondence and requests for materials should be addressed to M.L.L.

Competing financial interests

The authors declare no competing financial interests.